ASSOCIAÇÃO BRASILEIRA DE ENERGIA NUCLEAR – ABEN
2019 International Nuclear Atlantic Conference - INAC 2019
Santos, SP, Brazil, October 21-25, 2019

Agência Brasileira do ISBN
ISBN 978-85-99141-08-3
9 788599 141083

Mechanical-Structural Analysis of a Stainless Steel Fuel Rod Under Burst Test Conditions

Danilo P. Faria[1], Antonio T. e Silva[2], Leonardo S. Lima[1] and Jose R. Berretta[1]

[1] Centro Tecnológico da Marinha em São Paulo
Marinha do Brasil
05508-000 São Paulo, SP, Brazil
danilo.pinheiro@marinha.mil.br

2 Instituto de Pesquisas Energéticas e Nucleares
Universidade de São Paulo
05508-000 São Paulo, SP, Brazil
teixeira@ipen.br

ABSTRACT

After the Fukushima nuclear accident in 2011, the nuclear research community has initiated research into the development of fuels that are resistant to accidents. In this context, iron-based alloys have emerged as a good alternative to zirconium alloys. In order to make possible the cladding material replacement, studies related to their mechanical properties are necessary. Thus, the present study carried out a mechanical-structural evaluation from the available data collection regarding the mechanical properties of stainless steel 348, specifically in the conditions of the burst test. Burst tests were performed at various temperatures ranging from 32°C up to 450 °C. Then, a computational model was created based on the specimen of the burst test. Numerical simulation was performed considering the tensile tests of stainless steel at various temperatures. The numerical results were compared with the results of the burst test. Test and simulations were comparable leading to computational model validation. As austenitic stainless steels have structural stability for low and high temperatures, the results could be extrapolated to temperatures higher than those in the burst test. After the validation of the computational model, simulations were performed for temperatures higher than 450ºC, thus obtaining a burst pressure curve as a function of the temperature for stainless steel ANSI 348. The correlation of burst data as function of temperature could be implemented in the FRAPTRAN code, in order to make possible the evaluation of the behavior of a fuel rod with stainless steel ANSI 348 under postulated accident conditions (LOCA).

1. INTRODUCTION

Since 1968, zirconium based alloys have been the most used materials on fuel rods in commercial reactors. These alloys contain approximately 2.5% of tin and have properties

such as: good mechanical strength, high resistance to corrosion at high temperatures and low neutron capture cross sections to thermal neutrons [1].
The performance evaluation of fuel rods is fundamental for the licensing of nuclear fuel. This evaluation is done through experiments and computational codes that consider the different phenomena that occur throughout the fuel irradiation.
After the Fukushima nuclear accident in 2011, the nuclear research community has initiated research into the development of fuels that are resistant to accidents (ARF) aiming both the substitution of zirconium alloys as a cladding material and the increase of the thermal conductivity of the fuel insert, improving fuel performance in accident conditions [2]. In this context, iron-based alloys have emerged, as an alternative to zirconium alloys, since they have favorable mechanical properties and highly consolidated commercial production processes. Among the alloys based on iron, special attention has been given to the austenitic stainless steels of the 300 series, especially to the ANSI 348, because it was the cladding material used in the first PWRs, presenting good performance under irradiation [3,4].

2. METHODOLOGY

The present work has the objective of studying the mechanical properties, especially the burst at temperatures ranging from 25 to 1000ºC. This work was performed considering 3 steps, as described below.
Initially, the bursting test was carried out at different temperatures. However, it was not possible to continue the tests at temperatures above 450 °C, due to limitations the fluid used to compress the system. The computational model based on finite element using ANSYS software was developed in order to compare with burst experimental data performed previously. The computational simulation of burst experiment also requires mechanical properties data, which was obtained by means of additional tensile test performed at different temperatures.
Thus, from the validation of the computational model, the numerical results were extrapolated up to 800ºC and adjusted the burst pressure curve as a function of temperature for 348 stainless steel.

2.1. Burst Test

The experimental apparatus available for the burst test can be seen in Figure 1. The INSTRON machine uses oil to pressurize the line. The fluid introduced into the pressure line is the Mobiltherm 605 oil, indicated for use in high temperatures in closed systems. The furnace, which can operate up to 1000ºC, is controlled by 3 thermocouples in the lower, intermediate and upper part of the component.

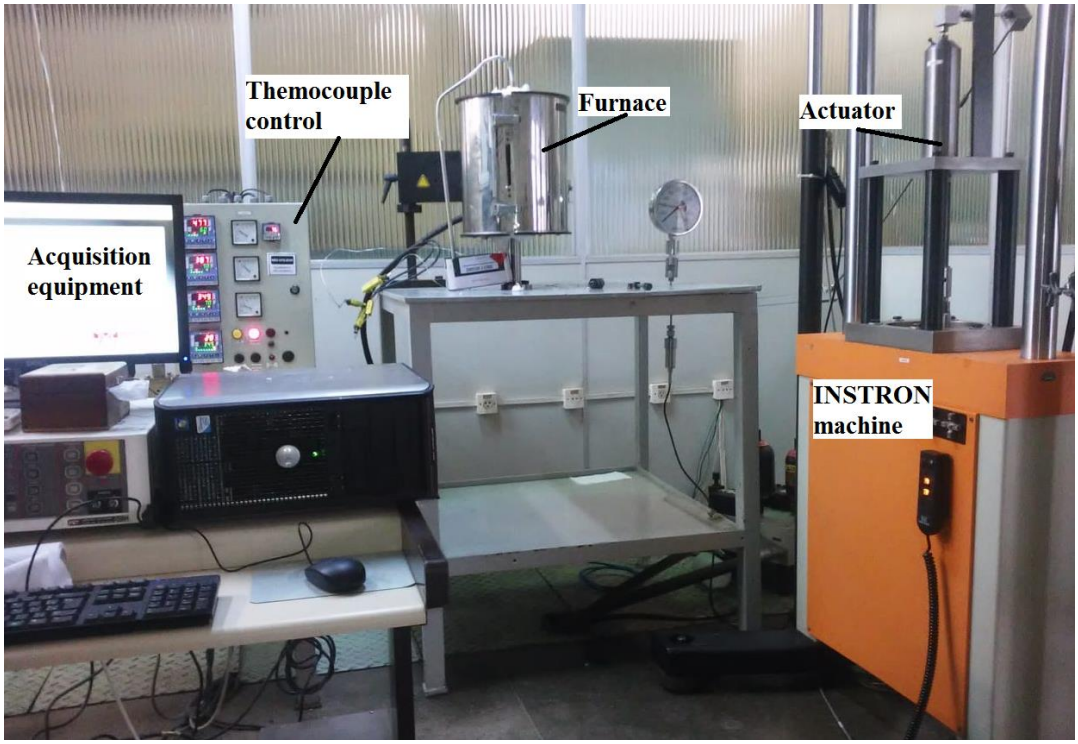

Figure 1 - Experimental apparatus for the burst test.

The bursting test and the preparation of the specimen complied with the ASTM B811 standard [5]. The actuator speed was 4.9 mm/min, calculated according to the ASTM. The sample was fixed at the end of the pressure line and positioned inside the furnace, as can be seen in detail in Figure 2.

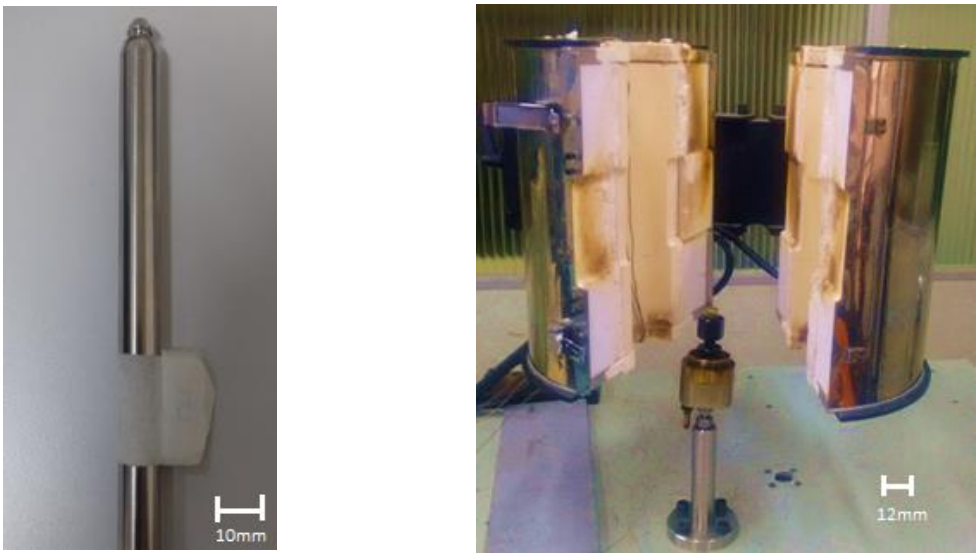

(a) (b)

Figure 2 - Detail of the specimen in the pressure line. (a) Sample; b) Detail of the pressure line end.

The burst tests were performed at four temperatures. The major limiting of the test was the fluid, which is inherent in the available experimental apparatus. Although the manufacturer requires that the oil could be used at 315ºC maximum, however was noted a risk of fire only with temperatures above 450ºC. Thus, tests were performed at room temperatures (25ºC), 150ºC, 370ºC and 450ºC, with 5 specimens analyzed at each level. Each sample was 160 mm long, 10 mm external diameter and 0.6 mm thickness.

2.2. Tensile Test

The experimental apparatus available for the tensile test is shown in figure 3 and figure 4.

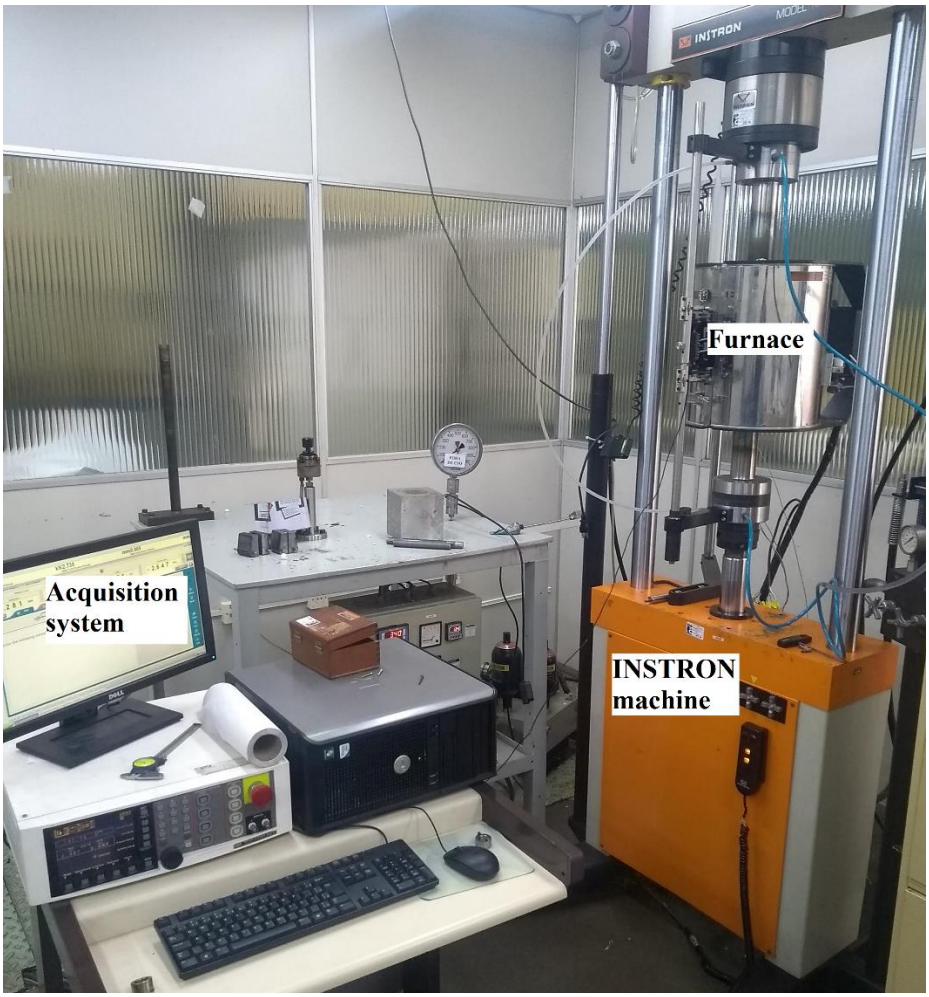

Figure 3 - Experimental apparatus for tensile test on the INSTRON Testing Machine.

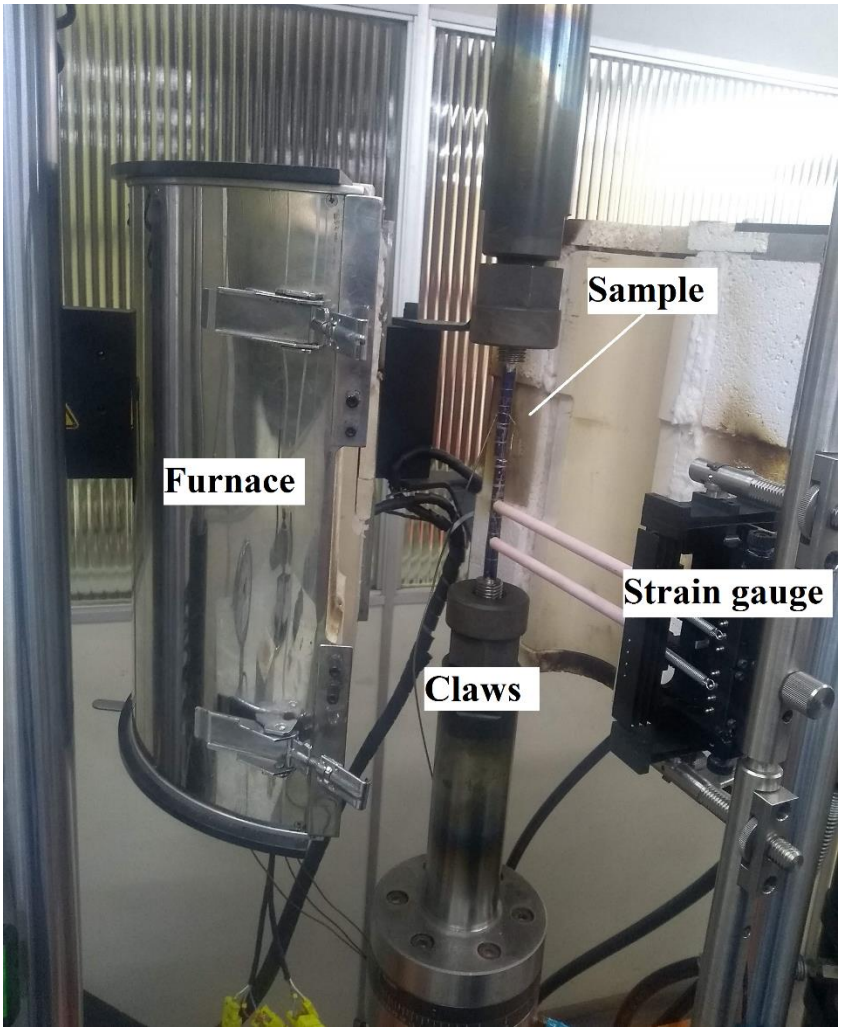

Figure 4 - Detail of the sample assembly in INSTRON.

The experimental procedure of the tensile test followed the ASTM E8/E8M standard [6]. Six temperatures were specified for the assay: 25 ºC, 150 ºC, 370 ºC, 450 ºC, 600 ºC and 800 ºC, and, for each of them, 5 samples were tested.

2.3. Computational Simulation

The computational model, planned in the $SOLIDWORKS^{®}$ program (v.18), was designed to reproduce the sample of Figure 2 (a). After the geometry design, the model was exported to the $ANSYS^{®}$ program (v.15) and discretized in FEM (Finite Element Method), as can be observed in Figure 5.

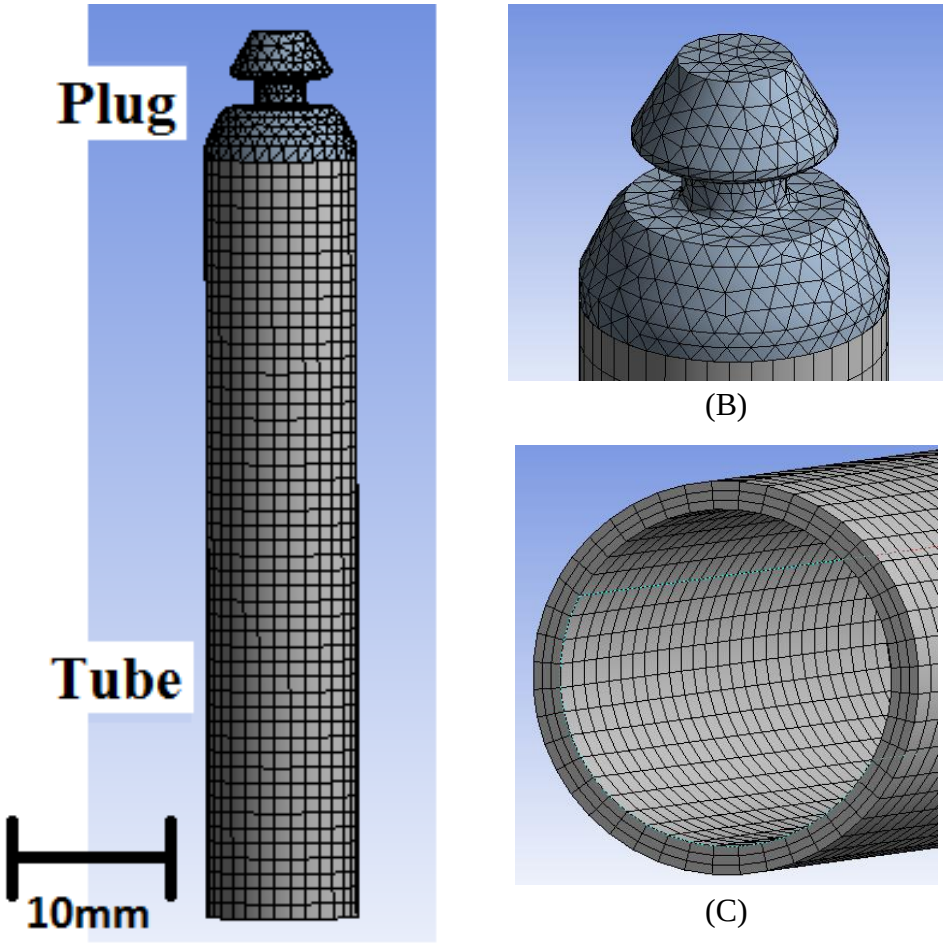

Figure* 5 - *Computational model discretized in FEM. A) Complete model. B) Plug detail. C) Tube detail.

The finite elements mesh was created as a function of the geometry: tetrahedral elements were used in the plug and hexagonal elements, with 3 elements in the thickness (see figure 5), in the tube. The boundary condition connecting the plug and the tube was chosen as bonded, representing the weld between the components.

The reliability of the numerical simulation is directly related to the veracity of the mechanical properties of the selected material for model's materials. Since in the literature data available properties as flow limit, maximum elongation, modulus of elasticity, resistance limit and yield limit, were slightly divergent from the mechanical properties of stainless steel ANSI 348 more accurate data was obtained through the test described in 2.2 section.

For the numerical simulation, a new material was created in the software's library. The material elastoplastic behavior was approximated for the bi-linear model and the mechanical properties were inserted for each temperature of interest.

The numerical simulation was developed in the "explicit dynamics" module of the ANSYS software, where calculations are performed explicitly from time-loading increments.

The criterion used to determine the bursting pressure of the model was the ultimate tensile strength of the material, as suggested in Massey et al [7]. Thus, it was considered as burst

pressure the pressure that generates a stress equivalent to the ultimate tensile of material at a given temperature. Numerical simulations were carried out at the following temperatures: 25ºC, 150ºC, 370ºC, 450ºC, 600ºC and 800ºC.

2.4. Results

After the burst test, the results of Table 1 were obtained, where P is the burst pressure.

Table 1: Experimental results of the burst test at different temperatures

Samples	P_25ºC [MPa]	P_150ºC [MPa]	P_370ºC [MPa]	P_450ºC [MPa]
1	71.3	55.9	50.3	48.6
2	69.5	55.8	52.6	48.8
3	69.1	55.9	50.5	48.9
4	70.9	56.8	51.6	47.9
5	70.5	53.7	51.0	49.1
Average [MPa]:	70.3	55.6	51.2	48.7
Standard deviation [MPa] :	0.9	1.1	0.9	0.5

The tensile test results, useful for providing material data for the numerical simulation, can be seen in Table 2.

Table 2: Results of the tensile test at different temperatures.

	Temperatures					
Properties	**25 ºC**	**150 ºC**	**370 ºC**	**450 ºC**	**650 ºC**	**800 ºC**
S_esc [MPa]	319.0	271.0	241.0	209.0	204.0	15.0
S_max [MPa]	646.0	493.2	454.0	444.0	386.8	210.0
elong_%	49.9	31.8	26.3	19.7	17.2	20.8
E [GPa]	200.0	190.0	17.0	168.0	154.0	143.0

Legend:
S_esc: yield strength.
S_max: tensile strength.
elong: elongation.
E: modulus of elasticity.

The Figure 6 shows, in detail, a sample test end at 800°C, illustrating an extreme condition of the equipment, with the specimen and the INSTRON claws in incandescent state.

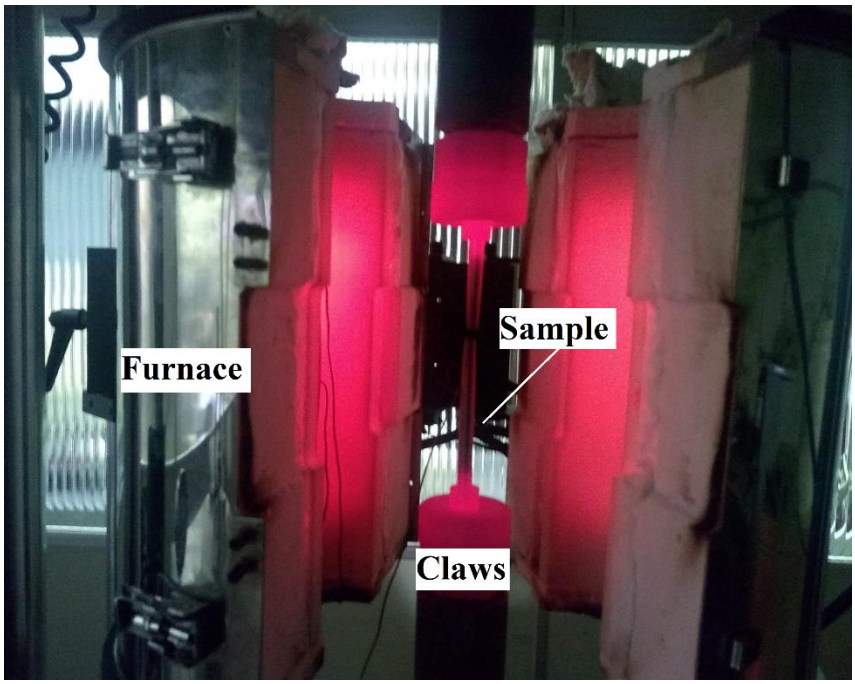

Figure 6: Tensile test at 800ºC.

Due to the limitation of the experiments, in temperature, it was only possible to validate the computational model for the test temperatures and then extrapolate the numerical results to temperatures higher than 450ºC. Figure 7 shows an example of stress distribution in the model as a function of the internal pressure applied.

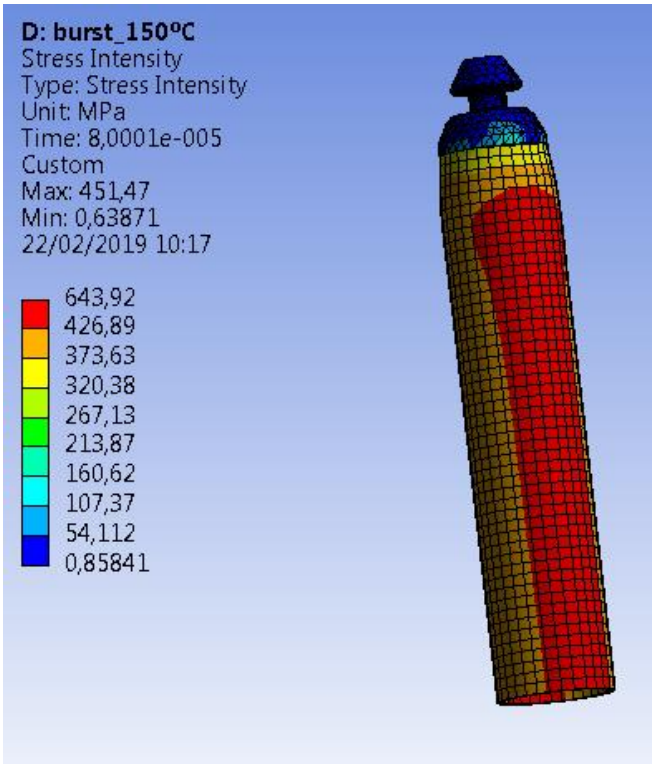

Figure 7: Example of a numerical simulation result at 150ºC.

The comparison of numerical and burst test results can be seen in Table 3, where P is the burst pressure.

Table 3 - Comparison between numerical and experimental results of burst pressure at different temperatures.

Temperature_ºC	P _experiment [MPa]	P_numeric [MPa]	Error %
32	70.26	69.91	0.50%
150	55.62	62.21	11,84%
370	51.20	51,34	0.27%
450	48.66	50.40	3.57%
		Mean Error:	**4.04%**

As shown in Table 3, the mean error between the numerical and experimental results was 4.2%. In this way, it can be considered that the computational model in the conditions described in 2.3 section was validated.

According to the references [8-11], the austenitic stainless steels have the capacity to maintain practically intact their crystalline structure at both low and high temperatures, which insures that the material has high mechanical strength even under extreme conditions. Thus, particularly for stainless steel, there is no abrupt change in structural behavior up to

the melting point of the material. Therefore, it is possible to use the computational model, for temperatures above 450ºC.
Table 4 complicit the numerical results up to 800ºC.

Table 4 – Numeric results of burst pressure.

Temperature [ºC]	Burst Pressure [MPa]
32	69.91
150	62.21
370	51,34
450	50.40
650	46.53
800	39.90

From the numerical and experimental results of Table 4 and Table 3 was plotted in chart, as can be observed in the Figure 9.

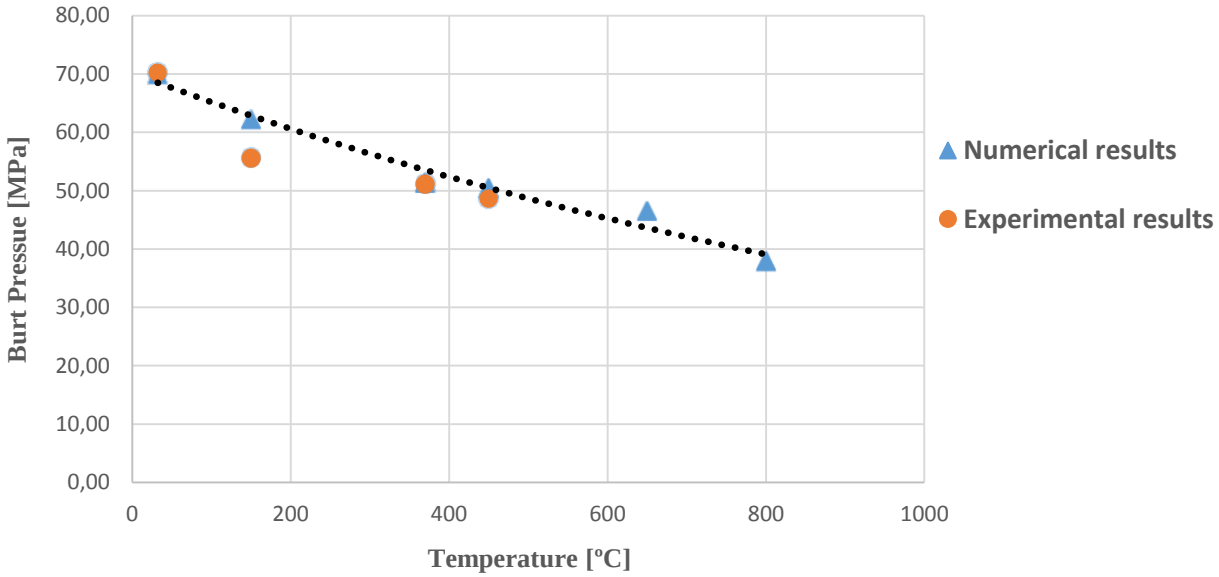

Figure 9 - Compilation of burst pressure results between numerical and experimental results.

In order to represent the behavior of the material was adjusted an exponential equation (see equation 1). The equation only covers numerical data. The calculated R^2 value was 0.968.

$$P = 70{,}129 * e^{-0{,}0007*T} \quad (1)$$

Legend:
P: Burst pressure [MPa]
T: temperature [°C]

3. CONCLUSIONS

In agreement with the results presented, it can be concluded that the methodology used for was successful, since the computational model built was validated from the comparison with the experimental results.
The exponential equation found was adjusted to numerical results with R^2 value greater than 0.96, which gives good reliability for its use.
Thus, as a function of the uniformity of the structural mechanical behavior of the material as a function of temperature, the bursting pressure of the stainless steel 348 can be predicted to thermal levels ranging from room temperature to melting point.
However, it is worth noticing to carry out burst tests at temperatures above 450 ° C, as they will result in more data for the comparison between the numerical and experimental results. In this way, it can be verified that stainless steel 348 is a good candidate to substitute zircaloy in power reactors. Since, despite being less efficient in relation to the consumption of neutrons, it has better mechanical properties and structural stability at high temperatures.

REFERENCES

1. Mendes, N. M. F.; Duvaizem J. H.; et al, “Utilização do Zircaloy - 4 em ligas de Ti-13Nb-13Zr para aplicação como biomaterial.”, *Congresso Latino Americano de Órgãos Artificiais e Biometria*, Natal-RN, 22-25 de agosto, pp. 1-2, (2012).

2. Abe, A.; Giovedi, C.; Gomes D. d. S. and Silva, A. T., "Revisiting Stainless Steel as PWR Fuel Rod Cladding after Fukushima Daiichi Accident", *Journal of Energy and Power Engineering*, pp. 1-4, (2014).

3. Shannon, B. S., "Development of advanced accident tolerant fuels for commercial LWRs", *Nuclear News*, pp. 83-87, (2014).

4. Giovedi, C.; Abe, A.; et al, "Assessment of Stainless Steel 348 Fuel Rod Performance Against Literature Available data Using Transuranus Code.", Nuclear Sciences & Tecnologies, pp. 1-8 (2016).

5. ASTM, B 811 "Standart Specification for Wrought Zirconium Alloy Tubes for Nuclear Reator Fuel Cladding", pp. 4-16, (2014).

6. ASTM, E8/E8M-13a " Standard Test Methods for Tension Testing of Metallic Materials", 2013.

7. Massey, C. P.; Terrani, K. A.; Dryepondt, S. N. and Pint, B. A.; "Cladding burst behavior of Fe-based alloys under LOCA", *Journal of Nuclear Materials*, **470,** pp.128-138, (2016).

8. Silva, I. L. A., "Efeito da Tempetarura na Microestrutura e Oxidação de um Aço Inoxidável Superduplex", *Universidade Federal do Norte Fluminense*, pp. 4-7, (2010).

9. Barbosa, P. A. D. , "Desenvolvimento de Aços Inoxidáveis Resistentes às Fluência", *Mestrado integrado em Engenharia Metalúrgica e de Materiais*, pp. 1-39, (2013).

10. "Associação Brasileira de aço inoxidável, aço inox: entenda por que ele é capaz de resistir a temperaturas extremas", https://www.abinox.org.br/site/agenda-inox-noticias-detalhes.php?cod=5865&q=A%25C3%25A7o+inox%253A+entenda+por+que+ele+%25C3%25A9+capaz+de+resistir+a+temperaturas+extremas, (2018).

11. Chiaverini, V., "Aços Carbono e Aços Ligas", *Boletim de Geologia e metalurgia*, **16ª Edição**, pp. 151-171, (1954).